

Modelling and Optimization of Orientated Beam with Tip Mass for Vibration Energy Harvesting using Piezoelectric Patches

Laxmi. B. Wali^{1*} and C V Chandrasekhara²

^{1*}Assistant Professor, Department of Mechanical Engineering, RNSIT, VTU, Bengaluru, Karnataka, India.

E-mail: laxmibwali@gmail.com

²Professor, Design Lead, Department of Mechanical Engineering, PES University, Bengaluru, Karnataka, India.

E-mail: drcvc@pes.edu

Abstract

Energy harvesting is extracting energy from ambient sources. Vibration energy harvesting area have received attention of many researchers to power wireless sensors and low-power electronic devices from smart materials. In literature, authors have focused on analytical and finite element models of cantilever beam with tip mass. The paper focuses on the novel numerical technique for orientated cantilever beam bounded with piezoelectric patches and mounted with tip mass using the direct method with non-orthonormalisation to derive the frequency response function (FRF) for voltage, current and power output. MatLab programme is developed considering the Euler Bernoulli beam assumptions, constitutive equations of piezoelectric material and Hamilton's principle. The MatLab programme is validated with the previous work on orthonormalisation electro-mechanical finite element for unimorph beam and good agreement is obtained. The dynamic characteristics of considered model is presented and optimized parameters are obtained.

Keywords: Orientation, Fem, Vibration, Energy harvesting, Piezoelectric.

1.0 Introduction

In the recent years, many researchers are attracted towards the area of energy harvesting from various sources available in the surrounding environment [1]. Energy from vibration is one of source which is available freely from machines, human motion having low frequency vibration excitation which can be used to meet the demand without depending on conventional sources. Research in the area of energy harvesting is increasing with the development of smart electronic devices. Limitation in batteries capacity to power the devices and life span for supplying continuous energy for wireless technologies necessitate for energy harvesting.

Smart structures based on piezoelectricity are currently generating a demand and piezoelectric material forms the alternate source for the creation of lifelong energy harvesters with compact configuration which will be utilized in engineering and medical applications. Research of piezoelectric elements in energy conversion applications necessitates a thorough understanding of solid mechanics and geometrical shapes [2]. Researchers have focused on analytical and numerical studies of unimorph and bimorph beam which forms the basis for the study of energy harvesting [3-5] due to its compatibility and ease of applications. Authors have studied experimentally, the effect of orientation of beam by attaching harvester to human leg and concluded that optimum results are obtained for 70°

*Corresponding Author

orientation of harvester with reference to coordinate system [6]. Researchers have focused on orientation of harvester for rotational motion by changing the distance between the rotating center and fixed end of beam [7]. A study on configurations of energy harvester for IoT sensor applications in smart cities [8] and optimal location of piezoelectric patch on the length of slat in aircraft applications is carried [9, 10]. A less information is available in the literature on the study of orientation of the beam with tip mass on free end and base excitation at fixed end. The aim of this work is to develop the MatLab programme for the study of orientation of the beam with tip mass, to study voltage, current and power frequency response function of the oriented cantilever beam bounded with piezoelectric patches mounted with tip mass and describe its dynamic behaviour and obtain the optimized parameters. The MatLab programme is validated with the previous work on orthonormalisation electro-mechanical finite element for unimorph beam and good agreement is obtained.

2.0 Methodology

The finite element method plays the major role in the complex problem analysis. In vibration based energy harvesting, piezoelectric unimorph beam forms the basic structure. The formulation of beam with piezoelectric (PZT) layer is considered as shown in Fig.1.

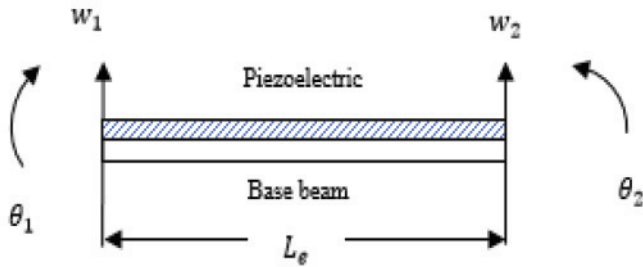


Figure 1: Element with base beam bounded with PZT

The beam with piezoelectric has two degree of freedom at each node, transverse (w) and rotational (θ)

The displacement function of the beam element is given as

$$w(x) = c_0 + c_1x + c_2x^2 + c_3x^3 \quad \dots (1)$$

Eqn. 1 is the displacement equation with four unknown coefficients. Applying boundary conditions at node 1 and 2 of element, the four coefficients in polynomial equation are solved.

The shape functions are given in equation (2-5)

$$[N] = [N_1 \quad N_2 \quad N_3 \quad N_4]$$

Where

$$[N_1] = \left(1 - 3 \left(\frac{x}{L_e} \right)^2 + 2 \left(\frac{x}{L_e} \right)^3 \right) \quad \dots (2)$$

$$[N_2] = \left(L_e \left(x - 2 \left(\frac{x}{L_e} \right)^2 + \left(\frac{x}{L_e} \right)^3 \right) \right) \quad \dots (3)$$

$$[N_3] = \left(3 \left(\frac{x}{L_e} \right)^2 - 2 \left(\frac{x}{L_e} \right)^3 \right) \quad \dots (4)$$

$$[N_4] = \left(L_e \left(- \left(\frac{x}{L_e} \right)^2 + \left(\frac{x}{L_e} \right)^3 \right) \right) \quad \dots (5)$$

Strain $S(x)$ is represented by

$$S(x) = -z \frac{d^2w(x)}{dx^2} = -zB \quad \dots (6)$$

$$B = [B_1, B_2, B_3, B_4]$$

Differentiating Eq. (2-5)

$$\frac{d^2N_1}{dx^2} = \frac{-6}{L_e^2} + \frac{12x}{L_e^3} = B_1 \quad \dots (7)$$

$$\frac{d^2N_2}{dx^2} = \frac{-4}{L_e} + \frac{6x}{L_e^2} = B_2 \quad \dots (8)$$

$$\frac{d^2N_3}{dx^2} = \frac{6}{L_e^2} - \frac{12x}{L_e^3} = B_3 \quad \dots (9)$$

$$\frac{d^2N_4}{dx^2} = \frac{-2}{L_e} + \frac{6x}{L_e^2} = B_4 \quad \dots (10)$$

The electro-mechanical coupling of a piezoelectric can be demonstrated in two ways. In direct piezoelectric effect, an applied mechanical pressure produces a proportional voltage response and in converse effect, an applied voltage produces a deformation of the material.

The direct effect Eq.11 and the converse effect Eq.12 may be modeled as

$$\{D\} = [e]^T \{S\} + [\varepsilon^S] \{E\} \quad \dots (11)$$

$$\{T\} = [c^E] \{S\} - [e] \{E\} \quad \dots (12)$$

The constitutive equation for 1-dimensional form with constant electric field and strain

$$\begin{Bmatrix} T_1 \\ D_3 \end{Bmatrix} = \begin{bmatrix} c_{11}^E & -e_{31} \\ e_{31} & \varepsilon_{33}^S \end{bmatrix} \begin{Bmatrix} S_1 \\ E_3 \end{Bmatrix} \quad \dots (13)$$

The base beam and piezoelectric plane stress field equation is given by Eq.14 and 15

$$T_1^{(1)} = c_{11}^{(1)} S_1^{(1)} \quad \dots (14)$$

$$T_1^{(2)} = c_{11}^{(2)} S_1^{(2)} - e_{31} E_3 \quad \dots (15)$$

$\vartheta(z) = \frac{z-z_n+h_p}{h_p}$ is the shape function over the interval $z_n - h_p \leq z \leq z_n$

$$z_n = \frac{c_{11}^{(1)} h_s^2 + c_{11}^{(2)} h_p^2 + 2c_{11}^{(1)} h_s h_p}{2(c_{11}^{(1)} h_s + c_{11}^{(2)} h_p)} \text{ distance from the}$$

neutral axis to the top layer of the beam with piezoelectric

$$\varphi(z) = \vartheta(z) v_p \text{ is electrical potential}$$

$$\Omega(z) \text{ first derivative of shape function} = \frac{d\vartheta(z)}{dz} = 1/h_p$$

The electric field equation

$$E_3 = -\Omega(z) v_p \quad \dots (16)$$

where v_p = voltage

Substituting Equation (6) into Equation (14)

$$T_1^{(1)} = -z c_{11}^{(1)} B \quad \dots (17)$$

Substituting Equation (6) and (16) into Equation (15)

$$T_1^{(2)} = -z c_{11}^{(2)} B + e_{31} \Omega(z) v_p(t) \quad \dots (18)$$

$$D_3 = -z e_{31} B - \varepsilon_{33}^S \Omega(z) v_p \quad \dots (19)$$

The electro-mechanical piezoelectric cantilever energy harvesting is formulated by the Hamiltonian principle,

$$\int_{t_1}^{t_2} [\delta(k - \beta + \omega) + \delta\omega] dt = 0 \quad \dots (20)$$

Representation of equations in matrix form utilizing extended Hamilton's principle [3]

$$\begin{bmatrix} M & 0 \\ 0 & 0 \end{bmatrix} \begin{Bmatrix} \ddot{w} \\ \ddot{v}_p \end{Bmatrix} + \begin{bmatrix} C & 0 \\ P_{sr} & P_D \end{bmatrix} \begin{Bmatrix} \dot{w} \\ \dot{v}_p \end{Bmatrix} + \begin{bmatrix} K & P_{rs} \\ 0 & 0 \end{bmatrix} \begin{Bmatrix} w \\ v_p \end{Bmatrix} = \begin{Bmatrix} F \\ i_p \end{Bmatrix} \quad \dots (21)$$

Element Stiffness Eq.22, mass matrix Eq.23 is given by

$$[K] = \int z^2 c_{11}^{(1)} [B^T] [B] dv^{(1)} + \int z^2 c_{11}^{(2)} [B^T] [B] dv^{(2)} \dots (22)$$

$$[M] = \int \rho^{(1)} [N^T] [N] dv^{(1)} + \int \rho^{(2)} [N^T] [N] dv^{(2)} \dots (23)$$

Adding tip mass terms to Eq. (23)

$$2I_0^{tip} x_c \frac{d[N^T]}{dx} + I_0^{tip} [N^T] [N] + I_2^{tip} \frac{d[N^T]}{dx} \frac{d[N]}{dx} \quad \dots (24)$$

Offset distance from proof mass centroid [5] is

$$x_c = \frac{\rho^{tip} b l_{tip}^2 h_{tip} + \rho^{(1)} b l_{tip}^2 h_s}{2(\rho^{tip} b l_{tip} h_{tip} + \rho^{(1)} b l_{tip} h_s)} \quad \dots (25)$$

Zeroth and second mass moment of inertia [5] is given by

$$I_0^{tip} = \rho^{tip} b l_{tip} h_{tip} + \rho^{(1)} b l_{tip} h_s \quad \dots (26)$$

$$\begin{aligned} I_2^{tip} &= \left(\rho^{tip} b l_{tip} h_{tip} \left(\frac{l_{tip}^2 + h_{tip}^2}{12} \right) \right. \\ &+ \rho^{tip} b l_{tip} h_{tip} \left(z_n - h_p + \frac{h_{tip}}{2} \right)^2 + \left(\frac{l_{tip}}{2} \right)^2 \left. \right) \\ &+ \left(\rho^{(1)} b l_{tip} h_s \left(\frac{l_{tip}^2 + h_s^2}{12} \right) \right. \\ &+ \rho^{(1)} b l_{tip} h_s \left(-z_n - h_p + \frac{h_s}{2} \right)^2 \left. \left(\frac{l_{tip}}{2} \right)^2 \right) \end{aligned} \quad \dots (27)$$

Damping matrix C is given as

$$C = \alpha M + \beta K \quad \dots (28)$$

Mechanical Force F is given by

$$F = -Q \ddot{w}_{base} \quad \dots (29)$$

Where

$$Q = \int \rho^{(1)} N^T dV^{(1)} + \int \rho^{(2)} N^T dV^{(2)} \quad (30)$$

Adding tip mass terms to Eq. (29)

$$-I_0^{tip} x_c \frac{d[N^T]}{dx} - I_0^{tip} [N^T] \quad (31)$$

Electromechanical coupling is given by

$$P_{sr} = - \int z \Omega(z)^T e_{31} B dV^{(2)} \quad \dots (32)$$

Capacitance matrix is given by

$$P_D = - \int \Omega(z)^T \varepsilon_{33} \Omega(z) dV^{(2)} \quad \dots (33)$$

Transformation matrix is given by

$$T = [\cos(\theta) \ 0 \ 0 \ 0; \ 0 \ 1 \ 0 \ 0; \ 0 \ 0 \ \cos(\theta) \ 0; \ 0 \ 0 \ 0 \ 1]$$

Formulating the Eq.(21) into global matrix based on electro-mechanical vector transformation. Voltage, current and power frequency response function obtained by direct non-ortho-normalised electro-mechanical dynamic equation is given by [5]

$$\begin{aligned} &\frac{v_p}{-\omega w_b e^{j\omega t}} \\ &= \left[j\omega C_p - \frac{1}{R_{load}} j\omega \Theta^T * [K - \omega^2 M + j\omega \zeta]^{-1} \Theta \right]^{-1} \dots (34) \\ &* j\omega \Theta^T [K - \omega^2 M + j\omega \zeta]^{-1} Q \end{aligned}$$

$$\begin{aligned} &\frac{i}{-\omega^2 w_{base} e^{i\omega t}} \\ &= \frac{1}{R_{load}} \left\{ [C_p i\omega + R_l - \Theta^T i\omega [-M\omega^2 + \zeta i\omega + K]^{-1} \Theta]^{-1} \dots (35) \right. \\ &* \Theta^T i\omega [-M\omega^2 + \zeta i\omega + K]^{-1} Q \left. \right\} \end{aligned}$$

$$\frac{P}{(-\omega^2 w_{\text{base}} e^{i\omega t})^2} = \frac{1}{R_{\text{load}}} \left\{ \left[C_p i\omega + R_1 - \Theta^T i\omega [-M\omega^2 + \zeta i\omega + K]^{-1} \Theta \right]^{-1} \dots (36) \right. \\ \left. * \Theta^T i\omega [-M\omega^2 + \zeta i\omega + K]^{-1} Q \right\}^2$$

The dynamic equations are solved assuming system response is linear under harmonic base excitation and beam is excited in transverse direction. The electro-mechanical piezoelectric cantilever energy harvesting beam equations are formulated by the Hamiltonian principle. The numerical work of the author [5] is extended to outline the key equations and include the tip mass and orientation for the electro-mechanical dynamic equation.

2.1 Model of Orientated Beam Bounded with Piezoelectric Patches and Tip Mass

The study on energy harvesting is carried on cantilever beam of length 'L'. The beam is divided into two parts L/2 each, L_p^1 and L_p^2 is the length of PZT patches, h_b and h_p is the thickness of base beam and PZT patch, θ is the orientation of second half part of beam bounded with PZT patch and mounted with tip mass.

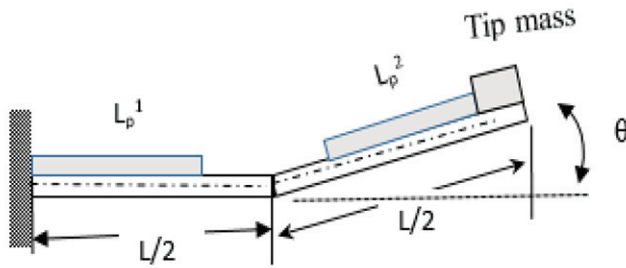


Figure 2: Orientation of Cantilever beam bounded with piezoelectric patches and tip mass at free end

Table 1: Geometry and material properties

Length, l	50e-3 (m)	Modulus of Elasticity of the PZT, E_p	66 (Gpa)
Width, b	6e-3 (m)	Density, $\rho^{(1)}$	9000 (kg/m3)
Thickness, h_b	0.5e-3 (m)	Density of the PZT layer, $\rho^{(2)}$	7800 (kg/m3)
Thickness of PZT, h_p	0.190e-3 (m)	Piezoelectric constant, e_{31}	-12.54 (C/m ²)
Modulus of Elasticity of the base beam, E_b	105 (Gpa)	Permittivity of constant strain, ϵ_{ps33}	1.3555e-008
Length of tip mass	15 (mm)	height of tip mass	10(mm)
Density of tip mass	9000 (kg/m3)	Damping constant	$\alpha=4.886$; $\beta=1.2433e-05$

The geometrical and material property of the beam are presented in Table 1. Tip mass is mounted on extended length of base beam. The length of the piezoelectric patches L_{p1} and L_{p2} is 20 mm each. The angle of orientations of the beam is 10° , 30° and 50° . The analysis of the beam is carried out using MATLAB programme in the frequency range of 0 to 1000 Hz. The cantilever beam is divided into 50 elements.

3.0 Results

The vibration energy in the environment occur with various frequencies. To exploit the vibration energy, the frequency of the model considered have to operate close to the vibration source. The importance to find the natural frequency is to obtain maximum output. The validation of the model is given in Tables 2 and 3

The MatLab programme is validated with material and geometrical properties of literature paper [3] and [5] and comparison of natural frequencies of unimorph piezoelectric energy harvester beam without tip mass and with tip mass at

Table 2: Comparison of Natural frequencies for unimorph beam without tip mass

Natural frequency	Literature paper [3]	MatLab results
1st	47.8	47.81
2nd	299.6	299.62
3rd	838.2	838.93

Table 3: Comparison of First natural frequency with tip mass

Literature paper [5]	MatLab results
18.5	18.48

0° orientation of beam is carried. The comparison of MatLab voltage FRF with the literature paper [4] is shown in Fig.3. As the resistance increases from 500 ohms to 1500 ohms, the voltage output increases.

The plot of Voltage, current and power FRF for the resistance of 500, 1000 and 1500 ohms is shown in Figures 4a, 4b and 4c. As the resistance increases from 500 to 1500 ohms, increase in voltage, current and power output is observed at 10° angle of orientation of second half of the beam.

Figure 5 shows the plot of natural frequencies verses orientation of second half part of beam. It is observed that as the angle

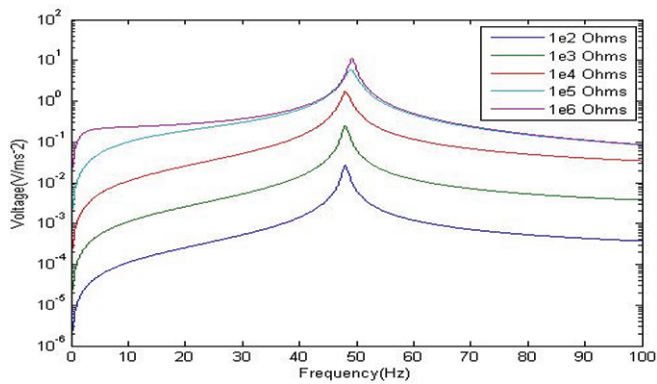


Figure 3: Plot of Voltage FRF

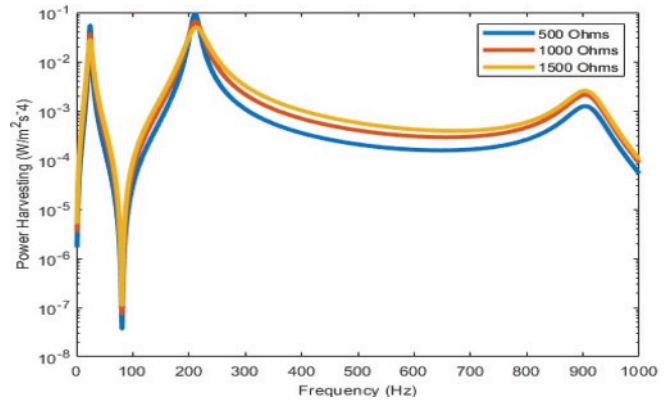


Figure 4: (c) Plot of Power FRF for beam with tip mass at 100 orientation

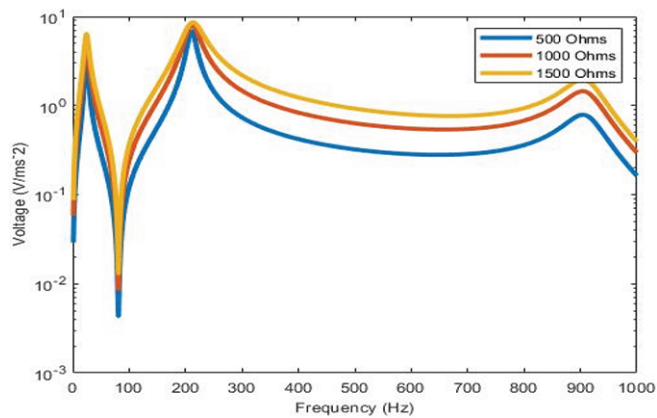


Figure 4: (a) Plot of Voltage FRF for beam with tip mass at 100 orientation

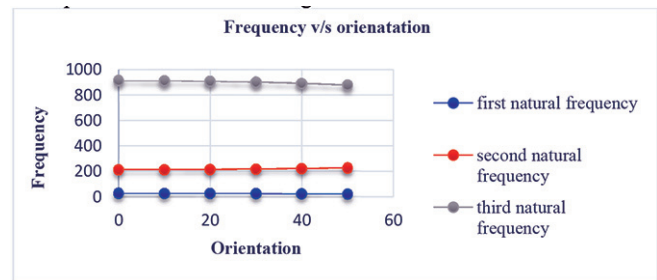


Figure 5: Plot of Natural frequencies versus orientation of beam

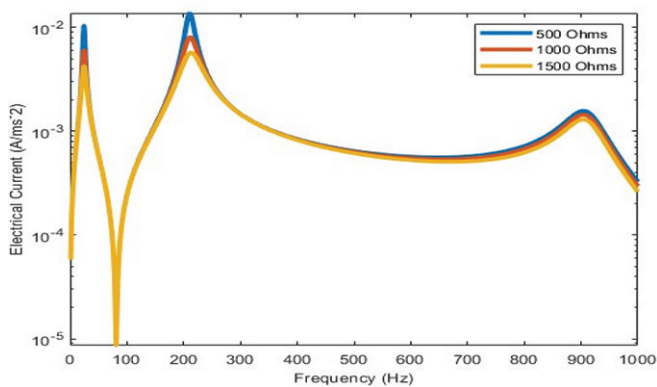


Figure 4: (b) Plot of Current FRF for beam with tip mass at 100 orientation

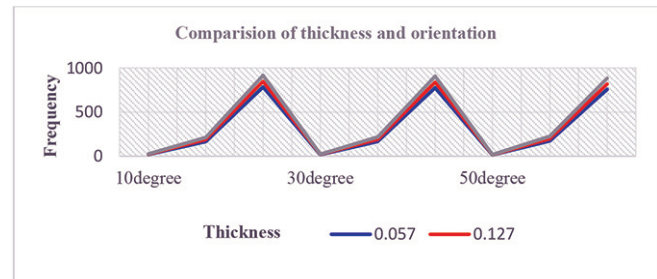


Figure 6: Plot of variation of thickness versus orientation

of orientation of beam increases from 10°, 30° and 50°, the first and third natural frequencies decreases with increase in second natural frequencies.

Figure 6 shows the plot of comparison of thickness of piezoelectric with orientation of beam. It is observed that as the thickness increases from 0.057 to 0.197 mm and angle of orientation from 10° to 50°, first and third natural frequency decreases with increase in second natural frequency.

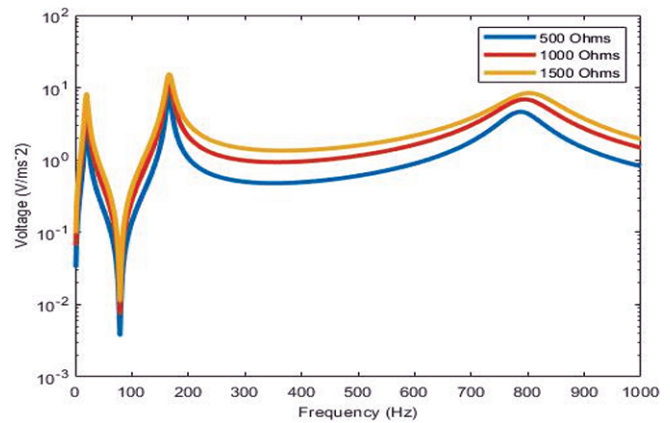


Figure 7: Plot of Voltage FRF

Figure 7 shows the plot of voltage FRF verses frequency for oriented beam with tip mass. The optimized voltage output is obtained at second natural frequency, when the beam orientation is at 10° and the thickness of piezoelectric is 0.057 mm at resistance of 1500 ohms.

5.0 Conclusions

MatLab programme is developed using finite element method considering the Euler Bernoulli beam assumptions, constitutive equations of piezoelectric material and Hamilton's principle. The paper focuses on the novel numerical technique for orientated cantilever beam bounded with piezoelectric patches and mounted with tip mass using the direct method with non-ortho-normalisation to derive the voltage, current and power frequency response function (FRF). It is observed that as the orientation increases from 0° to 50° , thickness of piezoelectric material from 0.057 to 0.197mm and resistance from 500 to 1500 ohms, the first and third natural frequencies decreases with increase in second natural frequencies and optimized voltage output is obtained at 10° orientation, 0.127mm thickness of piezoelectric and at resistance of 1500 ohms.

Nomenclature

$\{D\}$	Electric displacement vector
$\{T\}$	Stress vector
$[e]$	Dielectric permittivity matrix
$[c^E]$	Matrix of elastic coefficients at constant electric field strength
$\{S\}$	Strain vector
$[e^S]$	Dielectric matrix at constant mechanical strain
$\{E\}$	Electric field vector
I	Moment of inertia
Q	Charge
\ddot{w} base	Base excitation acceleration
Y	Young's modulus
κ	Kinetic energy
β	Potential energy
ω	Electrical energy
\overline{w}	External work
C_p	Trace of the global capacitance matrix
θ^T	Transformed electromechanical coupling
R_{load}	Resistance

K, M, ζ Global stiffness, mass and damping matrix
 ω Frequency

References

- [1] Shad Roundy, Paul K. Wright, Jan Rabaey A study of low level vibrations as a power source for wireless sensor nodes, *Computer Communications* 2003.
- [2] Henry A. Sodano and Daniel J. Inman A Review of Power Harvesting from Vibration using Piezoelectric Materials, *The Shock and Vibration Digest*. 2004; 36(3), 197-205.
- [3] A.Erturk , D. J. Inman A Distributed Parameter Electromechanical Model for Cantilevered Piezoelectric Energy Harvesters, *Journal of Vibration and Acoustics* 2008
- [4] Eziwarman, Mikail F. Lumentut. Comparative Numerical Studies of Electromechanical Finite Element Vibration Power Harvester Approaches of a Piezoelectric Unimorph. IEEE/ASME International Conference on Advanced Intelligent Mechatronics (AIM) Besançon, France 2014
- [5] Mikail F.Lumentut, Ian M.Howard Parametric design-based modal damped vibrational piezoelectric energy harvesters with arbitrary proof mass offset: Numerical and analytical validations, *Mechanical Systems and Signal Processing* 2016, 68-69 562-586
- [6] Iman Izadgoshasb et.al Optimizing orientation of piezoelectric cantilever beam for harvesting energy from human walking, *Energy Conversion and Management* 2018
- [7] Wei-Jiun Su et.al Analysis of a Cantilevered Piezoelectric Energy Harvester in Different Orientations for Rotational Motion, *Sensors* 2020 MDPI
- [8] Iman Izadgoshasb Piezoelectric Energy Harvesting towards Self-Powered Internet of Things (IoT) Sensors in Smart Cities, *Sensors* 2021 MDPI
- [9] Jiang Ding et.al A piezoelectric energy harvester using an arc-shaped piezoelectric cantilever beam array, *Microsystem Technologies* 2022
- [10] Domenico Tommasino et.al Vibration Energy Harvesting by Means of Piezoelectric Patches: Application to Aircrafts, *Sensors* 2022 MDPI